Ornithine-derived oligomers and dendrimers for in vitro delivery of DNA and ex vivo transfection of skin cells via saRNA

Francesca Saviano,[a] Tatiana Lovato,[b] Annapina Russo,[a] Giulia Russo,[a] Robin J Shattock,[c] Cameron Alexander,[b] Fabiana Quaglia,[a] Anna K. Blakney,[c]* Pratik Gurnani, [b]* Claudia Conte [a,]*

Abstract

Gene therapies are undergoing a renaissance, primarily due to their potential for applications in vaccination for infectious disease and cancers. Although the biology of these technologies is rapidly evolving, delivery strategies need to be improved to overcome the poor pharmacokinetics and cellular transport of nucleic acids whilst maintaining patient safety. In this work, we describe the divergent synthesis of biodegradable cationic dendrimers based on the amino acid ornithine as non-viral gene delivery vectors and evaluate their potential as delivery vectors for DNA and RNA. The dendrimers effectively complexed model nucleic acids at lower N/P ratios than polyethyleneimine and outperformed it in DNA transfection experiments with ratios above 5. Remarkably, all dendrimer polyplexes at N/P=2 achieved up to 7-fold higher protein content over an optimized PEI formulation when used for transfections with self-amplifying RNA (saRNA). Finally, transfection studies utilizing human skin explants revealed an increase of cells producing protein from 2% with RNA alone to 12% with dendrimer polyplexes, attributed to expression enrichment predominantly in epithelial cells, fibroblasts and leukocytes, with minor enrichment in NK cells, T cells, monocytes, and B cells. Overall, this study indicates the clear potential of ornithine dendrimers as safe and effective delivery vectors for both DNA and RNA therapeutics.

Introduction

Gene therapies are a powerful means to treat or cure disease, offering the possibility to introduce artificial genetic material into target cells, leading to the production or inhibition of disease-related proteins.[1] Although, gene therapy research has matured into some commercially viable technologies,[2] a number of challenges still remain in improving the efficacy of these therapies.[3] Due to the susceptibility towards nucleases and poor intracellular transport of naked nucleic acids, successful gene therapy relies on the efficient condensation, protection and delivery of genetic material using vectors. Typically, viral vectors outcompete non-viral delivery systems on transfection efficiency, however immunogenicity and manufacture issues have marred their clinical use.[4, 5]

There have now been a multitude of studies for the development of non-viral gene delivery vectors reported, typically comprising cationic lipids or cationic macromolecules, as formulation aids for nucleic acids.[6-12] They operate through the electrostatic condensation of negatively charged nucleic acids into small nanoparticles (lipoplexes for lipids, polyplexes for polymers), protecting the genetic material from endogenous nucleases.[13] It is now well established that the delivery vector must be explicitly tuned depending on the nucleic acid cargo, and that some vectors are more suitable for particular nucleic acid lengths.[14-16] This is particularly important as gene therapies can vary from short oligonucleotides (< 25 bases),[17] to mRNAs (~1-2 kb) and long (~10 kb) self-amplifying RNAs (saRNA).[18] There are also further complications owing to the need for formulations to navigate the challenges associated with application dependent administration, such as intramuscular injection for vaccination.[19]

Although polymeric gene delivery vectors can be synthesized at scale and with relative ease, their broad molecular weight distribution may result in variability which is carried through to biological activity. Pioneered by Tomalia and co-workers, dendrimers are perfectly branched macromolecules with monomer units repeated over each dendritic generation. Compared with traditional macromolecules, their synthesis is non-trivial, often achieved through iterative divergent or convergent strategies.[20] However, their perfect molecular weight distribution ($Đ$ = 1.0), coupled with their high surface valency for ligand display, have drawn significant attention for healthcare applications due to their reproducible interactions with biological systems. The success of dendrimers within a biomedical context also extends to gene delivery, with numerous cationic derivatives, such as poly(amidoamine) (pAMAM), and polypropyleneimine (pPI) displaying reproducible and strong nucleic acid complexation coupled with high transfection efficiencies.[21-29]

The ABB' (A = COOH, B = α-NH_2, B' = side chain NH_2) nature of amino acids with protonatable amine-functional side chains (lysine, ornithine etc.) represent excellent building blocks for dendrimer synthesis. Moreover, the polypeptide structure, and amino acid degradation products impart good compatibility with cells and tissues and allow for *in vivo* degradation of the vector through peptide bond cleavage by proteases.

Given the popularity of linear poly(lysine) (pLys) in gene delivery studies,[30, 31] the analogous cationic pLys dendrimers have also been extensively explored. [32-36] However, to date, no dendritic macromolecules based on other similar amino acids have been reported for gene delivery applications. Intriguingly, there are now a number of studies indicating that linear poly(ornithines) display more effective nucleic acid condensation, and thus a 10-fold increase in transfection efficiency in an array of cell lines compared to linear poly(lysine), due to the removal of one carbon between the poly(peptide) backbone and pendant amine. [37, 38]

We therefore decided to investigate ornithine-derived materials and describe here the synthesis of cationic dendrimers based on an ornithine repeat unit and evaluate their potential as pDNA and saRNA delivery vectors. Dendrimers with increasing generation were synthesized through iterative additions via a divergent strategy from a hexamethylenediamine core, and then formulated with model calf thymus DNA and plasmid DNA to form polyelectrolyte complexes (polyplexes). Utilising formulations initially optimized by a rapid screening methodology,[39] we examined transfection efficiencies of pDNA and saRNA in 2D cell monolayers mediated by the ornithine dendrimers. Finally, we probed their capability to enhance saRNA transfection in human skin explants and investigated which cell types contributed to protein expression relative to those cells which internalized the RNA. The data combined show the potential for these materials to be used in gene delivery and especially in vaccine formulations.

Materials and Methods

Materials

All solvents were of analytic or HPLC grade and purchased from Sigma Aldrich or Fisher Scientific unless otherwise stated. All deuterated solvents were purchased from Sigma Aldrich. L-ornithine monohydrochloride, BOC anhydride, NaOH, hexamethylendiamine, HBTU, triethylamine, sodium citrate, tris-borate-EDTA, agarose, sodium chloride (NaCl), magnesium chloride ($MgCl_2$), branched polyethylenimine (PEI) (2.5 kDa) Tris-base, DNase I from bovine pancreas were used as received from Sigma Aldrich. Calf thymus DNA was provided by Invitrogen. Blue/orange loading dye and ethidium bromide solution were provided by Promega. The plasmid pEGFP N1 was synthesized as previously described[40]

Instrumentation

*^{1}H NMR spectr*oscopy

^{1}H-, ^{13}C-NMR, 2D-NMR (COSY, HSQC, HMBC) spectra were recorded at 25 °C on a Bruker Advance III 400 MHz spectrometer. All chemical shifts are reported in ppm (δ) referenced to the chemical shifts of residual solvent resonances of d_6-DMSO (2.50 ppm). MestReNova 6.0.2 copyright 2009 (Mestrelab Research S. L.) was used for analysing the spectra.

Dynamic light scattering and zeta-potential

The hydrodynamic diameter (d_H), polydispersity index (PDI) and zeta potential of polyplexes were determined on a Zetasizer Nano ZS (Malvern Instruments Ltd.). The polyplex dispersion was diluted in Milli-Q water at intensity in the range 10^4-10^6 counts/s and measurements were performed at 25°C.

Synthesis and characterisation

BOC protection of L-ornithine

L-ornithine monohydrochloride (4.25 g, 25.22 mmol) was dissolved in deionized water (40 mL) under vigorous stirring and cooled to 0°C through an ice bath. The initial pH of the solution (around 6) was adjusted to 9 through the addition of NaOH. Then BOC anhydride (12.35 g, 56.63 mmol) was dissolved in THF (10 mL) and added dropwise to the cooled solution. The reaction was allowed to warm up to room temperature and proceed for 60 hours. The progress of the reaction was monitored through a ninhydrin assay. At the end of the reaction, THF was evaporated under reduced pressure, and the remaining aqueous solution acidified with a 1 M solution of HCl until the solution reached pH 2. The water phase was then extracted with ethyl

acetate (3 x 15 mL), and the organic fraction dried over $MgSO_4$, filtered and the product was recovered after evaporation as a white solid.

^{1}H NMR (400 MHz, DMSO-d_6): δ 12.42 (s, 1H), 7.02 (d, *J* = 8.0 Hz, 1H), 6.76 (t, *J* = 5.7 Hz, 1H), 1.37 (d, *J* = 3.1 Hz, 18H).

General procedure for L-ornithine coupling

A general procedure for coupling BOC-Orn to hexamethylenediamine (synthesis of G1), or the previous generation dendrimers (synthesis of G2 and G3) is described as follows. Multifunctional amine (G0, G1, G2) and BOC-Orn were dissolved in DMF under vigorous stirring in a 50 mL round bottomed flask. 2-(1H-benzotriazol-1-yl)-1,1,3,3-tetramethyluronium hexafluorophosphate (HBTU) and triethylamine was added to the flask and the reaction was allowed to proceed for 24 h at ambient temperature. The protected dendrimer was precipitated from a 10% sodium citrate solution yielding a white precipitate, which was filtered and washed with diethyl ether.

General procedure for BOC deprotection

The protected dendrimer was dissolved in trifluoroacetic acid and stirred at ambient temperature for 2 h. The solution was concentrated under reduced pressure, and the deprotected dendrimer isolated *via* precipitation in diethyl ether.

Synthesis of G1

BOC-orn (BOC)-OH (3.1020 g, 9.34 mmol) was coupled to hexamethylendiamine (505.3 mg, 4.35 mmol) using the reaction procedure stated above, utilizing (2-(1H-benzotriazol-1-yl)-1,1,3,3-tetramethyluronium hexafluorophosphate (HBTU) (3.3808 g, 8.91 mmol in 20 mL of DMF) and trimethylamine (3.6 mL) as coupling agent and organic base respectively in 20 mL of DMF. The product was collected as a white powder. The protected G1 dendrimer (2.80 g, 3,76 mmol) was deprotected as stated above in trifluoroacetic acid (13 mL) and recovered as a yellow/brown sticky solid (yield 87%).

^{1}H NMR (500 MHz, DMSO-d_6) δ 8.52 (t, J = 5.6 Hz, 1H), 8.27 (d, J = 5.3 Hz, 3H), 7.96 (s, 3H), 3.75 (h, J = 6.0, 5.6 Hz, 1H), 3.15 – 3.06 (m, J = 6.6 Hz, 2H), 2.79 (dq, J = 13.9, 4.9, 4.1 Hz, 2H), 1.79 – 1.67 (m, 2H), 1.57 (p, J = 7.8 Hz, 2H), 1.43 (p, J = 6.4 Hz, 2H), 1.32 – 1.21 (m, 2H). ^{13}C NMR (126 MHz, DMSO-d_6) δ 168.46, 52.13, 39.74, 38.68, 29.23, 28.65, 26.51, 23.05.

Synthesis of G2

BOC-orn (BOC)-OH (279.7 mg, 0.81 mmol) was coupled to G1 (279.7 mg, 0.81 mmol) using the reaction procedure stated above, utilizing HBTU (2.3601 g, 6.22 mmol in 5 mL of DMF) and triethylamine (1.05 mL) as coupling agent and organic base respectively in 10 mL of DMF. The product was collected as a white powder. The protected G2 dendrimer (300 mg, 0.19 mmol) was deprotected as stated above in trifluoroacetic acid (5 mL) and recovered as a yellow/brown sticky solid (yield 82%).

^{1}H NMR (400 MHz, DMSO-d6) δ 8.65 – 8.54 (m, 2H), 8.25 (s, 5H), 8.07 (t, J = 5.5 Hz, 1H), 7.92 (s, 5H), 4.24 (q, J = 7.9, 7.4 Hz, 1H), 3.89 – 3.82 (m, 1H), 3.75 (t, J = 6.6 Hz, 1H), 3.19 – 3.06 (m, 1H), 3.09 – 3.02 (m, 1H), 3.01 (d, J = 6.6 Hz, 1H), 2.80 (t, J = 7.4 Hz, 4H), 1.73 (dt, J = 14.0, 6.6 Hz, 3H), 1.58 (tq, J = 23.0, 12.7, 10.1 Hz, 3H), 1.37 (t, J = 6.9 Hz, 2H), 1.23 (s, 2H). ^{13}C NMR (126 MHz, DMSO) δ 168.46, 52.13, 39.74, 38.68, 29.23, 28.65, 26.51, 23.05.

Synthesis of G3

BOC-orn (BOC)-OH (1.23 g, 3.69 mmol) was coupled to G2 (325.5 mg, 0.41 mmol) using the reaction procedure stated above, utilizing HBTU (1.63 g, 4.29 mmol in 10 mL of DMF) and triethylamine (1.0 mL) as coupling agent and organic base respectively in 10 mL of DMF. The product was collected as a white powder. The protected G2 dendrimer (234 mg, 0.19 mmol) was deprotected as stated above in trifluoroacetic acid (5 mL) and recovered as an off-white sticky solid (yield 78%). ^{1}H NMR (400 MHz, DMSO-d6) δ 8.75 – 8.55 (m, 1H), 8.24 (s, 2H), 8.11 (d, J = 15.2 Hz, 2H), 8.02 (d, J = 8.0 Hz, 2H), 4.38 – 4.09 (m, 1H), 3.83 (dq, J = 42.0, 6.5, 6.0 Hz, 1H), 3.11 (t, J = 7.1 Hz, 1H), 3.02 (s, 1H), 2.81 (q, J = 9.3, 8.2 Hz, 2H), 1.77 (dq, J = 12.2, 5.8 Hz, 2H), 1.68 – 1.55 (m, 3H), 1.54 – 1.44 (m, 1H), 1.37 (s, 1H), 1.23 (s, 1H). ^{13}C NMR (101 MHz, DMSO) δ 171.75, 52.12, 39.54, 39.33, 28.68, 23.09.

Buffering capacity

Polymer (1 mg of dendrimer or PEI) was dissolved in 10 mL of NaCl (0.1 M) and the pH was adjusted to 10 through addition of NaOH (0.1 M). The polymer solution was titrated with HCl (0.1 M) and the pH value of solution was measured until pH 5.

Formulation and characterization of DNA polyplexes

General procedure

Stocks solutions of dendrimers G1, G2, G3, PEI and calf thymus DNA were prepared at double the concentration required in the polyplexes in HEPES buffer (20 mM, pH 7.4). Complexes were prepared by mixing the solutions 1:1 to produce N/P ratio of 0.25; 0.50; 1; 2; 5; 10; 20. In order to allow polyplex formation, the solutions were stirred for 45 minutes at room temperature.

Size and zeta-potential analysis

Polyplexes for size and zeta-potential analysis were prepared at the above N/P ratios, with dendrimer/PEI concentrations fixed at 0.1 mg mL^{-1} with the DNA concentration varied for each N/P ratio. Size measurements were performed directly with the prepared polyplex solutions. For zeta-potential measurements, polyplex solutions were diluted 1:1 with 10 mM NaCl (aq).

Gel retardation assay

Polyplexes for gel retardation assays were prepared with a fixed DNA concentration of 200 ng mL^{-1}, with the dendrimer/PEI concentrations varied for each N/P ratio. 20 µL of polyplex and 4 µL loading dye (6x) were loaded on to a 1% agarose gel + GelRed in Tris-borate-EDTA 0.5x (TBE) buffer and subjected to electrophoresis for 45 minutes at 70V and visualized with an UV illuminator.

Plasmid DNA purification

Plasmid pEGFP-C1 was transformed into the Escherichia coli DH5 and propagated in LB medium overnight at *37°C*.[41]

MTT assay

HCT $116^{p53-/-}$ cells were obtained from the American Type Culture Collection, cultured at 37°C in a humidified atmosphere containing 5% CO_2 and grown continuously in DMEM supplemented with 10% FBS, 100 unit/mL penicillin and 100 µg/mL streptomycin. HCT $116^{p53-/-}$ cells were seeded onto 96-well plates (2×10^4 cells/well) and cultured in 200 µL of cell medium with FBS at 10%. After 24 h, cells were treated and incubated with PEI and G3 polyplexes for 24 h. In particular, polyplexes at 2, 5 and 10 N/P ratios were prepared and tested at DNA concentrations of 0.1 – 0.8 µg/ mL. Then, cell viability was evaluated as a function of mitochondrial activity using the MTT assay. The absorbance was measured at 570 nm using a microplate reader (Biotek Synergy H1 Hybrid multiplate reader).

In vitro DNA transfection

HCT $116^{p53-/-}$ cells were grown in 12-well plates until 80-90% confluent and were then treated with polyplexes complexed to pEGFP-C1 DNA plasmid (0.2 µg per well) which encodes for the green fluorescence protein (GFP). After 24 h of incubation, the medium was aspirated, cells were washed with cold PBS, harvested and lysed as previously described [42]. Total protein extracts (200 g) from samples were subsequently analyzed for the expression of transfected DNA by measuring the fluorescence of the GFP. The fluorescence was measured with a Cary Eclipse fluorescence spectrophotometer (Varian). Excitation and emission wavelengths were 488 and 507 nm, respectively. The amount of total protein in the cell extracts was quantified using the Bradford-assay as previously described [43]. Results were plotted as the GFP fluorescence intensity in cells normalized against the protein amount in the cell extracts.

In vitro transcription of saRNA

Self-amplifying RNA encoding the replicase derived from the Venezuelan Equine Encephalitis Virus (VEEV) and either firefly luciferase (fLuc) or enhanced green fluorescent protein (eGFP) was produced using *in vitro* transcription. pDNA was transformed into E. coli, cultured in 100 mL of LB with 100 µg/mL carbenicillin (Sigma Aldrich, UK) an isolated using a Plasmid Plus MaxiPrep kit (QIAGEN, UK). The concentration and purity of pDNA was measured on a NanoDrop One (ThermoFisher, UK) and subsequently linearized using MluI for 3 h at 37 ˚C. For *in vitro* transfections, capped RNA was synthesized using 1 µg of linearized DNA template in a mMessage mMachine™ (Ambion, UK) and purified using a MEGAClear™ column (Ambion, UK) according to the manufacturer's protocol. RNA for *ex vivo* experiments was prepared as previously described.[19] Uncapped RNA transcripts were synthesized using 1 µg of linearized DNA in a MEGAScript™ reaction (Ambion, UK) according to the manufacturer's protocol. Transcripts were then purified by overnight LiCl precipitation at -20˚C, pelleted by centrifugation at 14,000 RPM for 20 min at 4 ˚C, washed 1X with 70% EtOH, centrfigued for 14,000 RPM for 5 min at 4˚C, and then resuspended in UltraPure H_2O (Ambion, UK). Purified transcripts were then capped using the ScriptCap™ m^7G Capping System (CEllSCript, Madison, WI, USA) and ScriptCapt™ 2'-O-Methyltransferase Kit (CellScript, Madison, WI, USA) simultaneously according to the manufacturer's protocol. Capped transcripts were then purified by LiCl precipitation as detailed above, resuspended in UltraPure H_2O and stored at -80˚C until further use.

Preparation of saRNA polyplexes

Stock solutions were prepared by dissolving the polymers and RNA in molecular grade H_2O at a concentration of 1 mg/mL. Polyplexes were then prepared in a buffer of 20 mM HEPES and 5 wt.% glucose at N/P ratios of 2, 5 and 10.

In vitro transfection of saRNA polyplexes

Transfections were performed in HEK293T.17 cells (ATCC, USA) that were maintained in culture in complete Dulbecco's Modified Eagle's Medium (cDMEM) (Gibco, ThermoFisher, UK) containing 10% (v/v) fetal calf serum (FCS), 5 mg/mL L-glutamine and 5 mg/mL penicillin and streptomycin (ThermoFisher, UK). Cells were plated at a density of 50,000 cells/well in a 96 well plate 24 h prior to transfection. At the time of transfection, the media was completely removed and replaced by 50 µL of transfection media (DMEM with 5 mg/mL L-glutamine). 100 µL of the polyplex solution was added to each well and incubated for 4 h. Then, the media was replaced with cDMEM and the cells were allowed to culture for 24 hours, at which time 50 µL of media was removed and 50 µL of ONE-Glo™ D-luciferin substrate (Promega, UK) was added and mixed well by pipetting. The total volume was transferred to a white 96-well plate (Costar, UK) and analyzed on a FLUOstar Omega plate reader (BMG LABTECH, UK). Cy5-labelled saRNA was purchased from TriLink (USA).

Flow cytometry analysis of eGFP expression in human skin explants

Surgically resected specimens of human skin tissue were collected at Charing Cross Hospital, Imperial NHS Trust, London, UK. All tissues were collected after receiving signed informed consent from patients, under protocols approved by the Local Research Ethics Committee (MED_RS_11_014). The tissue was obtained from patients undergoing elective abdominoplasty or mastectomy surgeries and processed as previously described.[19] Upon arrival in the laboratory the subcutaneous layer of fat was removed and the tissue was excised into 1 cm^2 pieces. Explants were incubated at 37˚C with 5% CO_2 in 12-well plates with cDMEM, which was replaced daily. Explants were injected intradermally (ID) using a Micro-Fine Demi 0.3 mL syringe (Becton Dickinson, UK) with 5 µg of eGFP saRNA polyplexes. After 72 h, explants were digested into single cell suspensions by incubating in 2 mL of DMEM supplemented with 1 mg/mL collagenase P (Sigma, UK) and 5 mg/mL dispase II (Sigma, UK) for 4 h at 37 ˚C on a rotational shaker. Digests were then filtered through a 70 µm cell strainer and centrifuged at 1750 RPM for 5 min. Cells were then resuspended in FACS buffer (PBS + 2.5% FCS) and stained with Fixable Aqua Live-Dead Cell stain (ThermoFisher, UK) diluted at 1:400 in FACS buffer for 20 min. Cells were then washed and stained with a panel of antibodies to identify each cell type for 30 min. The antibody panel included CD3-V450 (BioLegend, UK), CD14-Qdot605 (BioLegend, UK), CD19-BV650 (BioLegend, UK), CD56-BV711 (BioLegend, UK), CD1a-PerCP-eFluor710 (BioLegend, UK), CD11c-PE (BioLegend, UK), CD90-PE-Cy7 (BioLegend, UK) and CD45-AF700 (BioLegend, UK). Cells were then fixed in 1.5% paraformaldehyde and refrigerated until flow cytometry analysis. Samples were analyzed on a LSRFortessa™ (BD Biosciences, UK) with FACSDiva software (BD Biosciences, UK) with

100,000 acquired cell events. Gating and analysis was performed in FlowJo Version 10 (FlowJo LLC, Oregon, USA).

t-SNE representation of flow cytometry data

t-Distributed Stochastic Neighbor Embedding (tSNE) analysis of unsupervised clusters of live cells was performed in FlowJo using 1000 iterations, a perplexity of 30, a learning rate of 15196, the Exact (vantage point tree) KNN algorithm and the Barnes-Hut gradient algorithm. Unsupervised clusters are shown in grey, whereas the gated cells are superimposed on top with green ($eGFP^+$), blue ($Cy5^=$) and red (cell phenotype).

Statistical analysis

Graphical and statistical analysis were performed in GraphPad Prism, version 8. Statistical differences were analyzed using either multiple t tests adjusted for multiple comparisons or one-way ANOVA with multiple comparisons, with $p<0.05$ used to indicate significance.

Results and discussion

Dendrimer synthesis and complexation with DNA

Dendrimers of three generations (G1-G3) were synthesized via a divergent iterative addition-deprotection strategy utilizing BOC-protected ornithine (BOC-Orn, Figure 1, Figure S2). Initially, two equivalents of BOC-Orn were coupled to a hexamethylenediamine scaffold (G0) via conventional HBTU chemistry and subsequently deprotected using TFA to produce G1. This process was repeated twice using 4 then 8 equivalents of Boc-Orn to prepare G2 and G3 respectively.

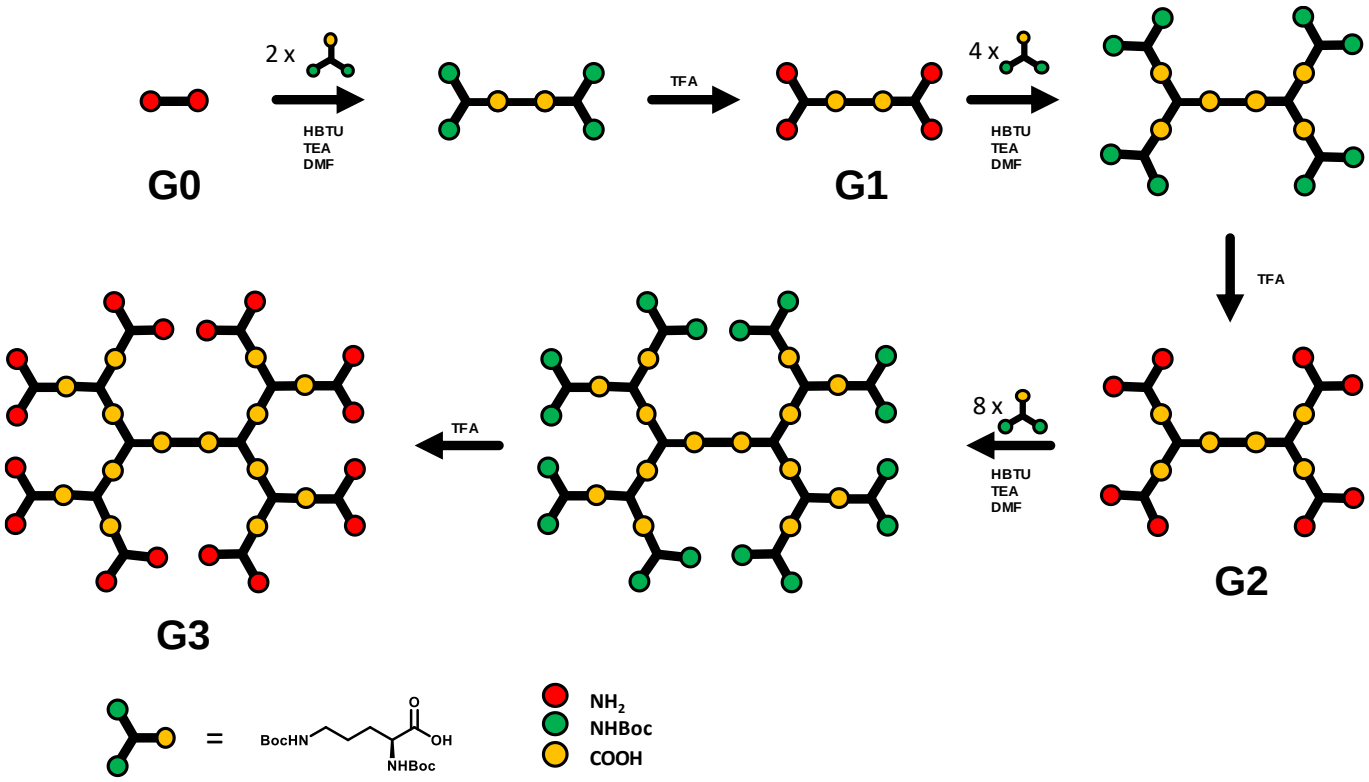

Figure 1. Representative iterative addition-deprotection divergent synthetic approach to produce ornithine dendrimers G1, G2 and G3 from Boc-protect ornithine and hexamethylenediamine (G0).

Deprotection reactions were confirmed by the disappearance of the singlet at ~1.5 ppm in ^{1}H NMR spectra for each dendrimer, whilst each iterative coupling was validated by the appearance of a signal at ~4.3 ppm attributed to the CH_2 protons next to the new amide bond (Figure 1, Figure S3, Figure S4).

The buffering capacities of dendrimers G1-G3 were determined through a pH titration and compared to PEI. All dendrimers (G1-G3) and PEI displayed some buffering compared to a NaCl solution. Within the family of dendrimers, it was observed that the buffering capacities increased with each generation of dendrimer, requiring 20, 50 and 90 µL of 0.1 M HCl to acidify the solution from pH 9 to pH 5 for G1, G2 and G3 respectively. This is likely due to the expanding number of ionisable nitrogens per generation, coupled with the increasing density of these groups which modifies the relative pK_a per each protonation event. None of the dendrimers displayed buffering comparable to PEI, however PEI has a very high density and greater number of protonatable amines than the relatively low molar mass dendrimers synthesised here (Figure 2A). The increasing buffering capacity with each successive generation of dendrimer might be expected to enhance endosomal escape, according to the 'proton sponge' hypothesis,[44] however, there have been some questions relating to the mechanisms by which polyplexes transport intracellularly,[45, 46] and thus we first required to evaluate nucleic acid binding and release properties outside a cellular environment.

To investigate the DNA binding capabilities of the cationic dendrimers, a range of dendrimer/DNA complexes at different N/P ratios (0.25 – 20) were formulated with G1, G2 and G3 with model calf thymus DNA (Figure S5). These polyplexes were compared to analogues prepared with PEI. All polyplexes prepared with PEI, G2 and G3 displayed particle sizes below 300 nm, however, dendrimer polyplexes had significantly lower PDI values than PEI, particularly at low N/P ratios. In contrast, G1 did not form stable polyplexes at any N/P ratio evidenced by their large sizes and negative zeta-potentials, probably due to the low polycation density. This was further supported by the lack of DNA retardation in the electrophoresis assay, in line with previous studies evaluating dendritic polylysine. Comparing between G2 and G3 polyplexes, the higher generation displayed smaller particle sizes, below 200 nm, potentially due to its greater charge density enabling greater electrostatic attraction, thus more efficient DNA condensation, in line with the most recent cationic materials investigated. G2 & G3 exhibited stronger binding capabilities of model calf thymus DNA than PEI, on the contrary of different PLL based polyplexes,[47] thus fully complexing the nucleic acid above N/P ratios 2 (compared to N/P 5 for PEI), as evidenced by the electrophoresis retardation assay. This is supported by the zeta-potential data which indicates the G2 and G3 polyplexes had positive potentials with lower polymer content (lower N/P ratio), compared to PEI which was negative until N/P 5. We postulate that this is due to the greater charge density on the dendrimer surface allowing for more efficient condensation than the conventional gaussian polymer chains of PEI.

Cytotoxicity and transfection of dendrimer-DNA polyplexes

The preliminary complexation studies suggested that the G3 poly(ornithine) materials were likely to be the most effective in transporting DNA into cells in 2D culture, owing to their smaller size relative to the other polymers in complexes with DNA. We selected a representative colon cancer cell line, HCT 116, as a target for these initial feasibility studies for nucleic acid transport. Accordingly, HCT $116^{p53-/-}$ cells were incubated with G3 and PEI polyplexes formulated at N/P 2, 5, 10, across four concentrations of pEGFP-C1 DNA plasmid (0.1 – 0.8 µg/mL). Cells treated with G3/pEGFP-C1 polyplexes exhibited excellent cell viability, above 90%. In contrast we observed some cytotoxic behaviour in cells treated with PEI polyplexes above 0.4 µg DNA at all N/P ratios (Figure 2B). In general, this suggests that G3 dendrimer polyplexes are significantly more biocompatible than those with PEI. This is likely due to the greater hydrophilicity of G3 than PEI, which is known to exhibit membrane damaging properties.

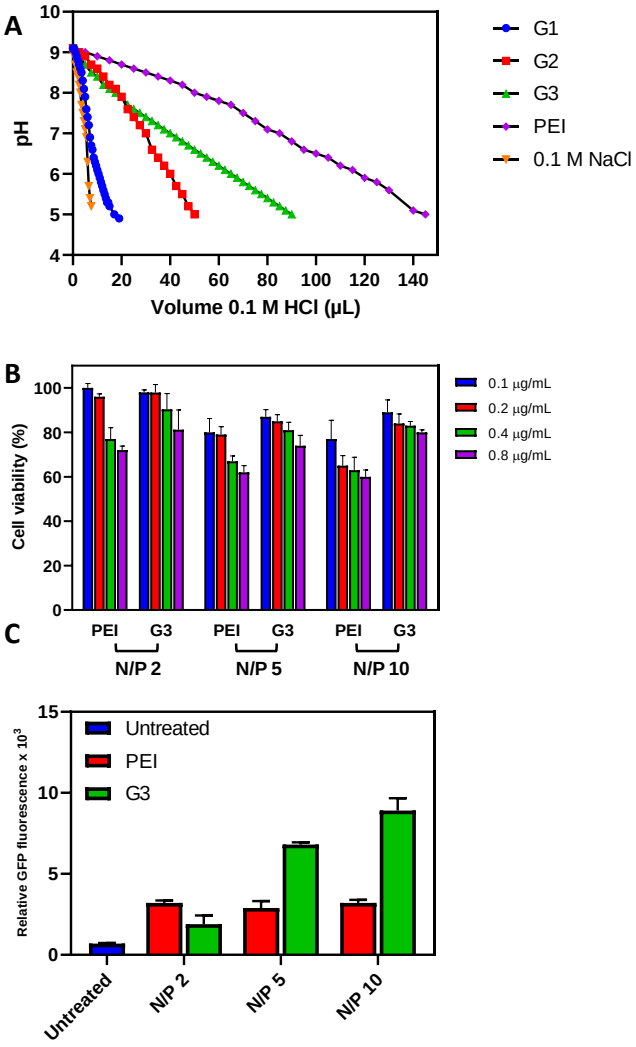

Figure 2. A) Potentiometric pH titration curves for dendrimers (G1, G2 and G3) and PEI, measured from pH 10 to 3 adjusting the pH with HCl (0.1 M). B) Cell viability of HCT 116 p53-/- cells after treatment with PEI and G3 pEGFP polyplexes at DNA concentrations of 0.1 – 0.8 µg/ mL. The cell viability from untreated cells was normalised to 100%. Results are presented as percentage (mean ± standard deviation) (n = 3) of the control cells. C) Transfection efficiency of PEI /DNA and G3 polyplexes/DNA at different N/P ratios using pEGFP-C1 plasmid in HCT 116p53−/− cells. Transfection efficiency of different delivery reagents was quantified by measuring the transgene expression level (GFP fluorescence intensity) 24 h after transfection by fluorescence spectroscopy. Results from three independent experiments (mean ± standard deviation) (n = 3) are displayed.

To evaluate transfection efficiency, HCT 116$^{p53-/-}$ cells were incubated with G3 or PEI polyplexes complexed to pEGFP-C1 (0.2 g), at N/P ratios 2, 5 and 10. After 24 hours, the transfection efficiencies were quantified by measuring the relative GFP expression by fluorescence spectroscopy in cell lysates (200 g). Although at N/P=2 G3 displayed lower GFP expression than PEI, the transfection efficiency was 2-3 fold higher in cells treated with G3 polyplexes at N/P ratio of 5 and 10 compared to PEI polyplexes. Interestingly, there was no correlation between GFP expression and N/P ratio for PEI polyplexes, whereas G3 polyplexes showed N/P ratio dependent expression, with higher ratios exhibiting more protein production (Figure 2C). This finding may be due to the observed cytotoxicity of PEI, which would limit total transfection efficiency, thus highlighting again a greater potential compared to the more employed PLL as gene delivery vector.[48]

In vitro transfection efficiency of self-amplifying RNA

For RNA vaccine applications, it is necessary to deliver the encoding nucleic acid to the cytosol and engage the translational machinery ultimately so that antigens expressed which induce an immune response. However, it is known that polycations alone can induce potent immune activation,[49] and thus we decided to evaluate G1-G3 polymers for delivery of saRNA even though the G1 and G2 complexes with the nucleic

acid were likely to be less stable than those of G3. In order to characterize the capacity of the dendrimers to deliver saRNA encoding for luciferase, we transfected HEK 293T.17 cells at N/P ratios ranging from 2-10 (Figure 3). PEI was used as a positive control at N/P=5, which was determined in the initial experiments to be the optimal ratio for this polymer with saRNA. We observed that ratios of N/P=2 resulted in the highest transfection efficiency (~10^5 RLU) for all three dendrimers (G1-G3), which were all significantly higher than the PEI control (~2 x 10^4 RLU, p=0.007, 0.014 and 0.00035, respectively). Interestingly, increasing the N/P to 5 and 10 for G1 did not impact the transfection efficiency, although both formulations were also significantly better at transduction of luciferase activity than PEI (p=0.044 and 0.00734, respectively). However, increasing the N/P for G2 and G3 inhibited the transfection efficiency. Overall, polymers G1-3 at N/P=2 induced the highest transfection efficiency, and further increasing the N/P ratio did not enhance luciferase expression. The higher transfection efficiencies at lower N/P ratios, and with the lower generation dendrimers (G1 and G2) may have been due to weaker electrostatic binding between these materials and RNA compared to those of higher mass and greater numbers of cationic residues. It thus may have been the case that for saRNA delivery, the polyplexes at higher N/P ratios and with higher charge densities (G3) were less efficient in release of the nucleic acid for translation into protein, resulting in a lower transfection efficiency.

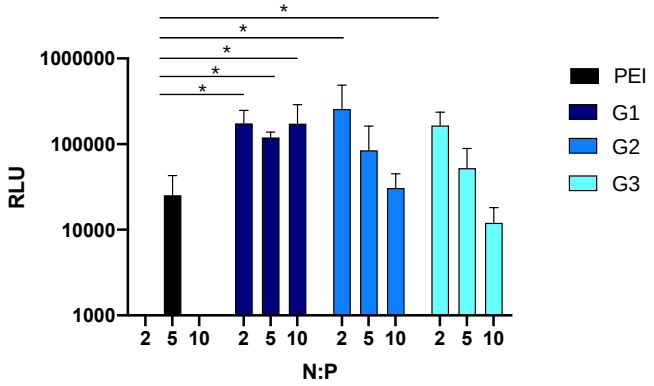

Figure 3. Transfection of polyplexes with saRNA encoding luciferase at N/P=2, 5 and 10 in HEK 293T.17 cells 24h after treatment. Bars represent mean ± standard deviation for n=3; * indicates significance of p<0.05 as determined by multiple t tests adjusted for multiple comparisons.

We, and others, have observed efficient RNA transfection by low-medium molar mass carriers.[39] In addition, a second mechanism relating to transfection may have been involved. The initial complexation studies revealed that G1 polymers did not form persistent and stable polyplexes with model DNA, as measured by light scattering. However, it is possible that weak complexation occurred at low N/P ratios and that transport of loose polymer-RNA aggregates nevertheless took place efficiently into the cellular interiors. Polymer G1 may also have had a role in aiding mRNA delivery by permeabilizing cellular membranes, enhancing either its internalization or translocation from intracellular compartments into the cytosol, in line with many prior studies describing the effects of polycations on biological membranes.[50, 51]

Transfection efficiency of saRNA/dendrimer polyplexes in *ex vivo* human skin explants

We then sought to characterize the ex vivo transfection efficiency of the dendrimers in human skin explants (Figure 4) using saRNA encoding for green fluorescent protein (GFP). Based on the *in vitro* transfection results Figure 3) we elected to use N/P ratios of 2 and 10, using RNA alone and PEI as controls. We observed that RNA alone resulted in GFP expression in ~2% of cells, and that complexation with PEI did not increase the number of GFP^+ cells. However, complexation of saRNA with G1-3 at N/P=2 resulted in ~7% of cells being positive for GFP expression. When G1 and G2 were increased to N/P=10 the number of GFP+ increased to ~12%, and was significantly higher than RNA alone or PEI, with p=0.011 and 0.003, respectively. There was no increase in the percentage of GFP^+ cells when the ratio for G3 was increased to N/P=10. These results are not in direct alignment with the *in vitro* transfection results; however, this is often the case for different transfection systems. The skin explants are a three-dimensional co-culture of many different cell types in a native tissue architecture as opposed to a monoculture of cells on a two-dimensional polystyrene surface. We subsequently analyzed *which* cells were expressing GFP in the skin explants (Figure 4B-C). We observed that the cell phenotype in the skin was predominantly epithelial (~50%), with

leukocytes (~10%) and fibroblasts (~12%), and a much smaller proportion of Langerhans cells (~5%), NK cells (~5%), dendritic cells (<1%), monocytes ~2%), B cells (~2%) and T cells (~1%) (Figure 4B). We observed that RNA and PEI formulations were expressed in similar populations, the majority of which were still epithelial cells, fibroblasts and leukocytes, but showing some enrichment in NK cells, T cells, monocytes, and B cells compared to the composition of the resident skin cell population (Figure 4C). G1 showed expression enrichment in fibroblasts and Langerhans cells, which was augmented by increasing the N/P ratio from 2 to 10. Interestingly G2 and G3 both showed an enrichment in epithelial cells, and to a lesser extent NK cells and Langerhans cells. Based on these observations we can conclude that G1 and G2 at N/P=10 enhance the percentage of cell expressing GFP in human skin explants, specifically in resident NK cells, Langerhans cells and epithelial cells.

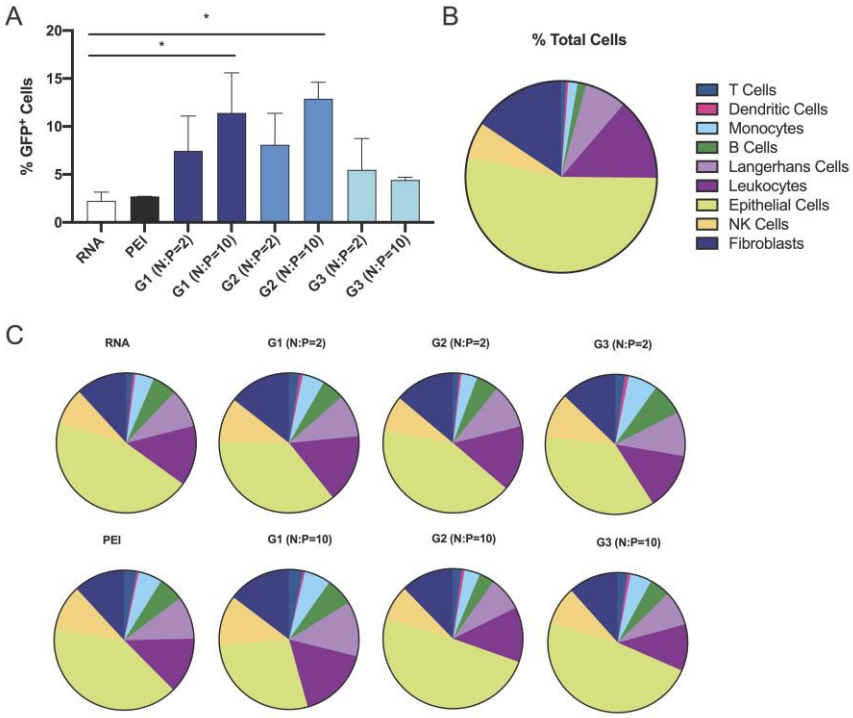

Figure 4. Cellular expression of saRNA after ID injection with polyplex formulations. A) Percentage of eGFP+ cells out of total live cells for each formulation after an intradermal injection of 5 µg of saRNA in human skin explants. Explants were analyzed 72 h after initial injection. Jet PEI was formulated at ratios of N/P = 5, while dendrimer formulations were prepared at ratios of N/P=2 or 10. Bars represent mean +/- SD for n = 3, with * indicating significance of $p < 0.05$ using an ordinary one-way ANOVA. B) Phenotypic identity of cell present in human skin explants and C) GFP+ cells after intradermal (ID) injection of polyplex formulations as determined by flow cytometry. Cells identified using the following antibodies: epithelial cells (CD45-), fibroblasts (CD90+), NK cells (CD56+), leukocytes (CD45+), Langerhans cells (CD1a+), monocytes (CD14+), dendritic cells (CD11c+), T cells (CD3+) and B cells (CD19+).

Characterization of polyplex uptake versus expression in human skin explants

Based on the observations that these dendrimers enhanced the percentage of GFP+ cells in human skin explants, we then wanted to explore how the formulation changed which cells internalised the polyplexes, compared to those cells which expressed the RNA. In order to probe this interaction we utilized Cy5 labelled saRNA that encodes eGFP, and analyzed the phenotypes using flow cytometry (Figure 5). We utilized t-distributed stochastic neighbor embedding (tSNE), to provide three-dimensional principal component analysis for flow cytometry data using unsupervised clustering. tSNE allows resolution of high-dimentional data arising from multi-paramter flow cytometry analysis into two dimensions, meanwhile preserving the structure of the data and revealing inherent clusters within the data.[52] The grey lines (Figure 5 A-B) indicate the tSNE unsupervised clustering, with $Cy5^+$ (blue) and $eGFP^+$ (green) gating applied on top, allowing for visualization of clusters of cells which internalised RNA, $Cy5^+$, and clusters expressing the RNA, $eGFP^+$. All the formulations yielded clusters of cells that had taken up RNA but were not expressing it, in addition to $eGFP^+/Cy5^+$ populations (Figure 5A). We then overlaid the gating for each cell phenotype in red to determine which white cells were responsible for uptake vs. expression (Figure 5B). We observed that T cells,

monocytes, B cells, Langerhans cells, leukocytes and NK cells internalised the RNA and expressed eGFP for each formulation. While there was uptake and expression in dendritic cells, there was a population of DCs in each formulation which was only positive for Cy5, indicating that these cells did not express the RNA to a detectable level. The epithelial cell and fibroblast populations for each formulation were also quite similar in that there was a higher proportion of these cells that were positive for RNA but which did not express GFP. Based on these observations we suggest that the uptake and subsequent expression of RNA varied in a phenotypic, not formulation dependent manner, and that increased expression relied on increasing the percentage of cells targeted by a formulation.

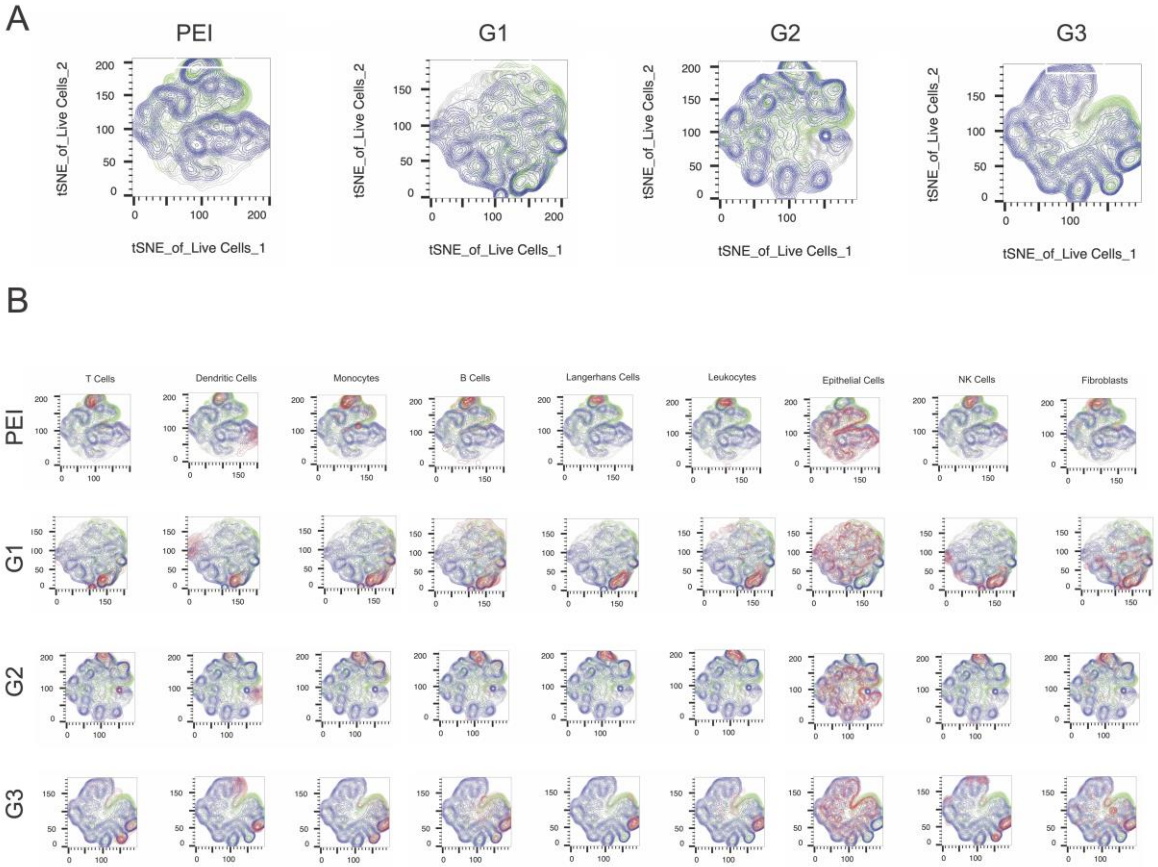

Figure 5. t-Distributed Stochastic Neighbour Embedding (t-SNE) analysis identifies cell populations that are positive for saRNA uptake (Cy5, blue) and saRNA expression (eGFP, green). A) t-SNE of live cells to show unsupervised clustering after injection with 5 µg of saRNA formulated with either PEI or dendrimers (G1-3). B) Overlay of phenotypic identification (red) as identified by cell gating overlaid with t-SNE.

Conclusions

In conclusion, this study demonstrates the potential for ornithine dendrimers as efficient non-viral delivery vectors for DNA and RNA, compared to the most popular cationic materials designed for gene therapy so far. G2 and G3 dendrimers outperformed the 'gold-standard' polymer in nucleic acid binding assays, complexing all available DNA at lower N/P ratios than PEI. Furthermore, the synthesized dendrimers exhibited significantly higher transfection efficiencies over PEI for DNA and RNA across 2D *in vitro* assays and 3D *ex vivo* skin explant studies. In skin, this increase was attributed to the dendrimer mediated enrichment in protein production in NK, Langerhans and epithelial cells, compared to RNA alone and PEI which displayed similar phenotypic protein expression. Finally using labelled RNA, we observed similar correlations between uptake and expression across each formulation. Somewhat surprisingly, in many of our transfection studies we observed significantly greater protein expression with the G1 and G2 dendrimers, which only contained 4 and 8 ionisable nitrogens, compared to 16 in G3. This potentially indicates that low generation dendrimers may be more effective for particular transfection settings than others. Given the data for efficient transfection in skin, we believe that some of these formulations may be effective vectors for RNA vaccines due to their substantial localisation with dermal immune cells. From a manufacturing perspective, these materials may alleviate potential batch-batch variability associated with macromolecules with non-uniform molecular weight distributions.

Conflicts of interest

There are no conflicts to declare.

Acknowledgements

This research is funded by the Department of Health and Social Care using UK Aid funding and is managed by the Engineering and Physical Sciences Research Council (EPSRC, grant number: EP/R013764/1). The views expressed in this publication are those of the author(s) and not necessarily those of the Department of Health and Social Care. This research was also funded through the Royal Society through a Wolfson Research Merit Award [WM150086]. C. Conte thanks the Italian Association for Cancer Research (AIRC) and the European Union (iCARE/Marie Curie 2014). F.Q., A.R. and G.R. wish to thank Regione Campania-POR Campania FESR for funding under 2014/2020 Project N. B61G18000470007. We also thank Douglas Crackett and Paul Cooling for expert technical assistance and Carol Turrill for outstanding administrative support.

Notes and references

1. K. A. High and M. G. Roncarolo, *New England Journal of Medicine*, 2019, **381**, 455-464.

2. L. DeFrancesco, *Nature Biotechnology*, 2019, **37**, 206-207.

3. H. Yin, K. J. Kauffman and D. G. Anderson, *Nature Reviews Drug Discovery*, 2017, **16**, 387-399.

4. D. Cross and J. K. Burmester, *Clinical medicine & research*, 2006, **4**, 218-227.

5. J. L. Shirley, Y. P. de Jong, C. Terhorst and R. W. Herzog, *Molecular Therapy*, 2020, **28**, 709-722.

6. Z. Y. Chen, W. Huang, N. Zheng and Y. G. Bai, *Polymer Chemistry*, 2020, **11**, 664-668.

7. Z. Y. Kang, Q. B. Meng and K. L. Liu, *Journal of Materials Chemistry B*, 2019, **7**, 1824-1841.

8. T. J. Gibson, P. Smyth, M. Semsarilar, A. P. McCann, W. J. McDaid, M. C. Johnston, C. J. Scott and E. Themistou, *Polymer Chemistry*, 2020, **11**, 344-357.

9. Z. M. Bai, J. Wei, C. M. Yu, X. S. Han, X. F. Qin, C. W. Zhang, W. Z. Liao, L. Li and W. Huang, *Journal of Materials Chemistry B*, 2019, **7**, 1209-1225.

10. Y. K. Sung and S. W. Kim, *Biomaterials research*, 2019, **23**, 8.

11. N. Veiga, M. Goldsmith, Y. Granot, D. Rosenblum, N. Dammes, R. Kedmi, S. Ramishetti and D. Peer, *Nature Communications*, 2018, **9**, 4493.

12. Y. N. Fan, M. Li, Y. L. Luo, Q. Chen, L. Wang, H. B. Zhang, S. Shen, Z. Gu and J. Wang, *Biomaterials Science*, 2018, **6**, 3009-3018.

13. T. F. Martens, K. Remaut, J. Demeester, S. C. De Smedt and K. Braeckmans, *Nano Today*, 2014, **9**, 344-364.

14. Z. P. Guo, L. Lin, J. Chen, X. Z. Zhou, H. F. Chan, X. S. Chen, H. Y. Tian and M. W. Chen, *Biomaterials Science*, 2018, **6**, 3053-3062.

15. Z. Meng, J. O'Keeffe-Ahern, J. Lyu, L. Pierucci, D. Z. Zhou and W. X. Wang, *Biomaterials Science*, 2017, **5**, 2381-2392.

16. R. Kedmi, N. Veiga, S. Ramishetti, M. Goldsmith, D. Rosenblum, N. Dammes, I. Hazan-Halevy, L. Nahary, S. Leviatan-Ben-Arye, M. Harlev, M. Behlke, I. Benhar, J. Lieberman and D. Peer, *Nature Nanotechnology*, 2018, **13**, 214-219.

17. H. Nam, S. H. Ku, H. Y. Yoon, K. Kim, I. C. Kwon, S. H. Kim and J. B. Lee, *Advanced Therapeutics*, 2019, **2**, 1900014.

18. A. K. Blakney, P. F. McKay, D. Christensen, B. I. Yus, Y. Aldon, F. Follmann and R. J. Shattock, *Journal of Controlled Release*, 2019, **304**, 65-74.

19. A. K. Blakney, P. F. McKay, B. Ibarzo Yus, J. E. Hunter, E. A. Dex and R. J. Shattock, *ACS Nano*, 2019, **13**, 5920-5930.

20. D. A. Tomalia, H. Baker, J. Dewald, M. Hall, G. Kallos, S. Martin, J. Roeck, J. Ryder and P. Smith, *Polym J*, 1985, **17**, 117-132.

21. J. Zhou, J. Wu, N. Hafdi, J. P. Behr, P. Erbacher and L. Peng, *Chemical communications*, 2006, DOI: 10.1039/b601381c, 2362-2364.

22. F. Abedi-Gaballu, G. Dehghan, M. Ghaffari, R. Yekta, S. Abbaspour-Ravasjani, B. Baradaran, J. E. N. Dolatabadi and M. R. Hamblin, *Applied materials today*, 2018, **12**, 177-190.

23. G. Navarro and C. Tros de Ilarduya, *Nanomedicine : nanotechnology, biology, and medicine*, 2009, **5**, 287-297.

24. D. Kaur, K. Jain, N. K. Mehra, P. Kesharwani and N. K. Jain, *J Nanopart Res*, 2016, **18**.

25. M. Hashemi, S. M. Tabatabai, H. Parhiz, S. Milanizadeh, S. A. Farzad, K. Abnous and M. Ramezani, *Mat Sci Eng C-Mater*, 2016, **61**, 791-800.

26. C. Dufes, I. F. Uchegbu and A. G. Schatzlein, *Advanced drug delivery reviews*, 2005, **57**, 2177-2202.

27. S. P. Chaplot and I. D. Rupenthal, *Journal of Pharmacy and Pharmacology*, 2014, **66**, 542-556.

28. Y. Dong, Y. Chen, D. Zhu, K. Shi, C. Ma, W. Zhang, P. Rocchi, L. Jiang and X. Liu, *Journal of Controlled Release*, 2020, **322**, 416-425.

29. D. P. Walsh, A. Heise, F. J. O'Brien and S. A. Cryan, *Gene Therapy*, 2017, **24**, 681-691.

30. M. Byrne, D. Victory, A. Hibbitts, M. Lanigan, A. Heise and S.-A. Cryan, *Biomaterials Science*, 2013, **1**, 1223-1234.

31. M. Yamagata, T. Kawano, K. Shiba, T. Mori, Y. Katayama and T. Niidome, *Bioorganic & Medicinal Chemistry*, 2007, **15**, 526-532.

32. B. J. Boyd, L. M. Kaminskas, P. Karellas, G. Krippner, R. Lessene and C. J. H. Porter, *Molecular pharmaceutics*, 2006, **3**, 614-627.

33. M. Gorzkiewicz, M. Konopka, A. Janaszewska, I. I. Tarasenko, N. N. Sheveleva, A. Gajek, I. M. Neelov and B. Klajnert-Maculewicz, *Bioorganic Chemistry*, 2020, **95**, 103504.

34. M. Ohsaki, T. Okuda, A. Wada, T. Hirayama, T. Niidome and H. Aoyagi, *Bioconjugate chemistry*, 2002, **13**, 510-517.

35. M. Männistö, S. Vanderkerken, V. Toncheva, M. Elomaa, M. Ruponen, E. Schacht and A. Urtti, *Journal of Controlled Release*, 2002, **83**, 169-182.

36. T. Okuda, A. Sugiyama, T. Niidome and H. Aoyagi, *Biomaterials*, 2004, **25**, 537-544.

37. E. Ramsay and M. Gumbleton, *Journal of drug targeting*, 2002, **10**, 1-9.

38. E. Ramsay, J. Hadgraft, J. Birchall and M. Gumbleton, *International journal of pharmaceutics*, 2000, **210**, 97-107.

39. T. Lovato, V. Taresco, A. Alazzo, C. Sansone, S. Stolnik, C. Alexander and C. Conte, *Journal of Materials Chemistry B*, 2018, **6**, 6550-6558.

40. A. Russo, S. Maiolino, V. Pagliara, F. Ungaro, F. Tatangelo, A. Leone, G. Scalia, A. Budillon, F. Quaglia and G. Russo, *Oncotarget*, 2016, **7**, 79670-79687.

41. A. Russo, G. Russo, M. Cuccurese, C. Garbi and C. Pietropaolo, *Biochimica et biophysica acta*, 2006, **1763**, 833-843.

42. A. Russo, A. Saide, S. Smaldone, R. Faraonio and G. Russo, *International journal of molecular sciences*, 2017, **18**.

43. D. De Filippis, A. Russo, A. D'Amico, G. Esposito, C. Pietropaolo, M. Cinelli, G. Russo and T. Iuvone, *British journal of pharmacology*, 2008, **154**, 1672-1679.

44. J. P. Behr, *Chimia*, 1997, **51**, 34-36.

45. R. V. Benjaminsen, M. A. Mattebjerg, J. R. Henriksen, S. M. Moghimi and T. L. Andresen, *Molecular Therapy*, 2013, **21**, 149-157.

46. S. Yang and S. May, *Journal of Chemical Physics*, 2008, **129**.

47. E. Mennesson, P. Erbacher, V. Piller, C. Kieda, P. Midoux and C. Pichon, *The journal of gene medicine*, 2005, **7**, 729-738.

48. L.-L. Farrell, J. Pepin, C. Kucharski, X. Lin, Z. Xu and H. Uludag, *European Journal of Pharmaceutics and Biopharmaceutics*, 2007, **65**, 388-397.

49. P. Lührs, W. Schmidt, R. Kutil, M. Buschle, S. N. Wagner, G. Stingl and A. Schneeberger, *The Journal of Immunology*, 2002, **169**, 5217-5226.

50. S. Lukasiewicz and K. Szczepanowicz, *Langmuir*, 2014, **30**, 1100-1107.

51. M. Soliman, R. Nasanit, S. Allen, M. C. Davies, S. S. Briggs, L. W. Seymour, J. A. Preece and C. Alexander, *Soft Matter*, 2010, **6**, 2517-2524.

52. L. Van Der Maaton and G. Hinton, *J. Mach. Learn. Res.*, 2008, **9**, 2579-2625.